

## Elucidation of the Role of the Complex in Hydride Transfer Reaction between Methylene Blue and 1-Benzyl-1,4-dihydrnicotinamide by Effect of $\gamma$ -Cyclodextrin

YINGJIN LIU, NAOTO HORIUCHI, YOSHIMI SUEISHI and SHUNZO YAMAMOTO\*  
Graduate School of Natural Science and Technology, Okayama University, 3-1-1, Tsushimanaka, 700-8530, Okayama, Japan

(Received: 18 April 2005; in final form: 30 May 2005)

**Key words:** hydride transfer reaction, reaction mechanism, cyclodextrin, inclusion complexes, 1-benzyl-1,4-dihydrnicotinamide, methylene blue

### Abstract

The kinetics of the hydride transfer reaction between Methylene Blue ( $\text{MB}^+$ ) and 1-benzyl-1,4-dihydrnicotinamide (BNAH) were studied in 10% ethanol-90% water mixed solvents containing  $\beta$ - and  $\gamma$ -cyclodextrins ( $\beta$ -CD and  $\gamma$ -CD). The pseudo-first order rate constant shows kinetic saturation at high initial concentration of BNAH. This indicates the formation of a complex between  $\text{MB}^+$  and BNAH. The reaction was suppressed by addition of  $\beta$ -CD, but enhanced by addition of  $\gamma$ -CD.  $\text{MB}^+$  and BNAH were separately accommodated within the  $\beta$ -CD cavity and the cavity walls may protect the activity site of the reactants. On the other hand, in the  $\text{MB}^+$ -BNAH- $\gamma$ -CD system, the inclusion of the complex between  $\text{MB}^+$  and BNAH with  $\gamma$ -CD occurred. This effect of  $\gamma$ -CD can distinguish between the productive and non-productive nature of the complex.

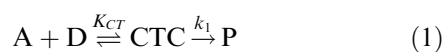
### Introduction

Cyclodextrins (CDs) possess cavities with a truncated cone shape with a nonpolar and hydrophobic interior and two hydrophilic rims formed by primary and secondary alcohol groups. CDs are capable of forming inclusion complexes by admitting guest molecules into their cavities [1]. Changes in the physico-chemical properties and reactivities result from such host-guest interactions. The effects of inclusion complexes on reactivities vary widely and depend on the guest, the CD, and the reaction [2,3].

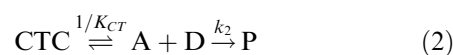
Hydride transfer reactions have been an attractive research topics *in vivo* as well as *in vitro* [4–6]. There has been considerable interest in understanding the reaction mechanisms of hydride transfer from various substrates to acceptors [7–12].

Ohno *et al.* [8] and Bunting *et al.* [13] suggested that charge-transfer (CT) complexes formed as intermediates between the reactants in some hydride transfer reactions. However, the mechanistic involvement of a CT complex has always been questioned by an alternative mechanism in which the CT complex acts as a bystander in an otherwise dead-end equilibrium. The two possible mechanisms are:

#### Mechanism-1



#### Mechanism-2



where A and D denote an electron acceptor and donor, respectively, CTC denotes a charge transfer complex, and P denotes a product. It was shown that the experimental rate constant  $k_{\text{exp}}$  is related to  $k_1$  and  $k_2$  as follows:

$$k_{\text{exp}} = \frac{k_1 K_{CT} [\text{A}]_0}{1 + K_{CT} [\text{A}]_0} \quad (3)$$

$$k_{\text{exp}} = \frac{k_2 [\text{A}]_0}{1 + K_{CT} [\text{A}]_0} \quad (4)$$

where  $K_{CT}$  is the equilibrium constant for the formation of the CT complex and  $[\text{D}]_0 \ll [\text{A}]_0$ . Since Equations (3) and (4) indicate that saturation curves can be obtained by plotting the values of  $k_{\text{exp}}$  against  $[\text{A}]_0$ , Mechanisms 1 and 2 are kinetically indistinguishable at constant temperature.

For mechanism 1, the rate of formation of P is expected to increase, while for mechanism 2 the rate to decrease with increasing CTC concentration. Therefore, if the concentration of CTC can be controlled by physical or chemical factors, we can distinguish between mechanism 1 and 2 by examining response of the rate to

\* Author for correspondence. E-mail: yamashun@cc.okayama-u.ac.jp

these factors. Since the formation of CTC generally exothermic, the concentration of CTC is decreased by increasing temperature. Negative and positive temperature dependence of the rate for the formation of P might be observed in mechanism 1 and 2, respectively. Unfortunately, in most hydride transfer reactions, however, the positive temperature dependence for  $k_1$  step overwhelms the negative temperature dependence for  $K_{CT}$  step, and eventually positive temperature dependence of overall rate for the formation of P was observed. As pointed out by Kiselev and Miller [14], the observation of negative activation enthalpy for the second order rate constant can be taken as experimental proof that the reaction passes through formation of CTC (mechanism 1). Recently, negative activation enthalpies were observed for some hydride-transfer reactions, and it was concluded that CT complexes act as real intermediates in these reactions [15–17].

Ueno *et al.* [18] observed that two molecules of 1-naphthyl acetate were accommodated within  $\gamma$ -CD cavity to form a ternary complex. It has been further reported that  $\gamma$ -CD includes the dimers of Methylene Blue [19,20], Acridine Orange [20], Roccellin [21], and Pyronine Y [22], etc.

Tan *et al.* [23] have reported that a ternary 1:1:1 inclusion complex was formed among  $\gamma$ -CD, 2,6-naphthalenecarboxylate ion, and 2,6-bis(1-pyridinylmethyl) naphthalene dibromide. Hamai has observed that ternary inclusion complexes between  $\gamma$ -CD and a 1:1 complex of thionine with 2-naphthalenesulfonate [24] and between  $\gamma$ -CD and a 1:1 complex of MB with 1-naphthol orange [25] were formed. The cavity of  $\gamma$ -CD is too large to fit some molecules and ions, but  $\gamma$ -CD forms stable inclusion complexes with their dimers or 1:1 complexes between them.

If  $\gamma$ -CD forms a stable ternary inclusion complex with CTC, the total concentration of CTC increases, and the rate of the formation of P is expected to increase and decrease in mechanism 1 and 2, respectively. Therefore, the effects of  $\gamma$ -CD on the rates of hydride transfer reactions would be taken another experimental proof for the speculation of role of CTC in them.

Sevcik and Dunford studied the kinetics of the oxidation of dihydronicotinamide adenine dinucleotide (NADH) by  $MB^+$  [26]. They obtained a saturation curve by plotting the observed rate constant against  $[NADH]_0$ , and proposed mechanisms which include the formation of a 1:1 complex between NADH and  $MB^+$ . However, they could not distinguish whether the complex was productive or nonproductive.

In hydride transfer reactions, 1-benzyl-1,4-dihydronicotinamide (BNAH) and related compounds have been regarded as model compounds of NADH [27]. Although the reaction mechanisms of hydride transfer reactions have been widely studied, little attention has been paid to the inclusion effects of CDs in hydride transfer reactions.

In this paper, we studied the effects of  $\beta$ - and  $\gamma$ -CD on the reaction of  $MB^+$  with BNAH in 10%

ethanol–90% water mixed solvents. The kinetic study of the effects of CDs on the rate of reduction of  $MB^+$  by BNAH is of interest in view of (1) whether CDs inhibit or promote the hydride transfer from BNAH to  $MB^+$ , and (2) whether detailed information on the mechanistic aspect of the reaction can be obtained.

## Experimental

### Materials

BNAH was obtained from Tokyo Kasei Kogyo Chemical Industry. Methylene Blue ( $MB^+$ ),  $\beta$ - and  $\gamma$ -cyclodextrins ( $\beta$ - and  $\gamma$ -CD) were purchased from Wako Pure Chemical Industries. These compounds were used as received. 10 vol% ethanol aqueous solutions of substrates were deaerated by bubbling 99.999% nitrogen gas for more than 20 min just before mixing.

### Kinetic measurements

The spontaneous decomposition of BNAH was observed in neutral or weakly basic solutions. We determined the rate constant for this spontaneous decomposition to be  $k_{sp} = 1.0 \times 10^{-4} \text{ s}^{-1}$  at pH = 7.5,  $k_{sp} = 1.4 \times 10^{-5} \text{ s}^{-1}$  at pH = 8.5 and  $k_{sp} = 2.7 \times 10^{-6} \text{ s}^{-1}$  at pH = 9.2 in glycine-KOH buffer at 25 °C. We have never observed any measurable decomposition of  $MB^+$  in buffers in the absence of BNAH. In all cases, conditions were chosen so that such background reactions occurred to an extent of less than 1% of the rate of the reduction of  $MB^+$  by BNAH.

The reactions were followed by recording the decrease in absorbance at 665 nm, due to the disappearance of  $MB^+$  under deaerated conditions, using a Shimadzu MultiSpec-1500 photodiode-array spectrophotometer. A typical kinetic procedure was as follows. The cuvette which contained BNAH solution of different concentrations in glycine-KOH buffer (pH = 9.2) in 10% ethanol–90% water (v/v) mixed solvents was capped with a rubber septum. Inlet and outlet needles were attached, and nitrogen (99.999%) was bubbled through the solution for at least 5 min. The cuvette was placed in a cell holder and thermostated. Previously deoxygenated  $MB^+$  solution was injected with a microsyringe into the cuvette. The initial concentration of  $MB^+$  was always  $1.0 \times 10^{-5} \text{ mol dm}^{-3}$  and the initial concentrations of BNAH were in 10-fold or larger excess over  $MB^+$ . The reaction was initiated by addition of a stock solution of  $MB^+$ . The absorbances were recorded till reaction completion. All the runs except for those in the presence of  $\gamma$ -CD gave good first-order plots over 3 half-lives. The absorption spectra of reaction mixtures in EPA (ethyl ether-pentane-ethanol) were measured at various temperatures with a Shimadzu MultiSpec-1500 photodiode-array spectrophotometer. The absorption spectra in the visible region at temperatures between 170 K and 240 K were consistent with that of  $MB^+$ .

It is well known that equilibrium between the  $\text{MB}^+$  monomer and its dimer exists in aqueous solutions. The equilibrium constant reported for  $\text{MB}^+$  dimerization is  $9600 \text{ mol dm}^{-3}$  [28]. Judging from the equilibrium constant about 7% of  $\text{MB}^+$  exists as the dimer at  $1.0 \times 10^{-5} \text{ mol dm}^{-3}$   $\text{MB}^+$  in aqueous solution. Since hydrophobic interactions are generally decreased by adding organic solvent to water, to reduce the portion of the dimer, 10% ethanol-90% water mixed solvent was used in this study.

## Results and Discussion

### Kinetics of the reduction of $\text{MB}^+$ by BNAH

The reaction of  $\text{MB}^+$  with BNAH, illustrated by Eq. (5), was studied in 10% ethanol-90% water mixed solvents under deaerated conditions.

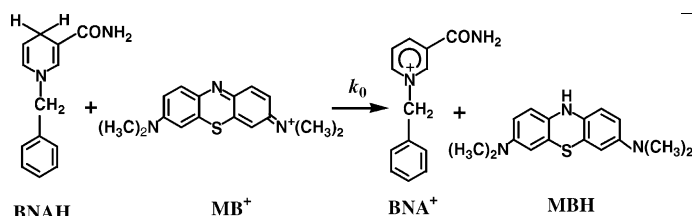


Figure 1 shows the time dependence of the absorption spectrum for the reaction of  $\text{MB}^+$  with BNAH. The time-dependent curves of the absorbance of  $\text{MB}^+$  at 665 nm showed that the absorbance gradually decreased after mixing  $\text{MB}^+$  solution with BNAH solutions of several initial concentrations, while the absorption of BNAH at 360 nm showed only slight decreases, because BNAH was in excess. Under these experimental conditions, more than 97% of  $\text{MB}^+$  changed to leuco Methylene Blue (MBH) (the  $\text{MB}^+$  concentrations were recovered almost quantitatively to the initial values on aeration of the reaction mixtures in which  $\text{MB}^+$  disappeared completely). Similar results were obtained for runs in the presence of CDs. It was found that the

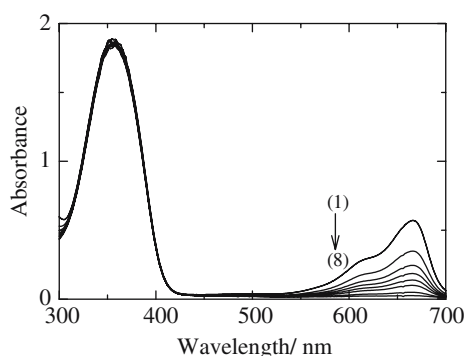


Figure 1. Repetitive scan of absorbance for the reaction of  $\text{MB}^+$  with BNAH in 10% ethanol-90% water mixed solvent at 298 K.  $[\text{MB}^+]_0 = 1.0 \times 10^{-5}$ ;  $[\text{BNAH}]_0 = 1.86 \times 10^{-4}$  M. Spectra were taken at (1) 5, (2) 75, (3) 120, (4) 160, (5) 200, (6) 240, (7) 340, and (8) 440 s after mixing.

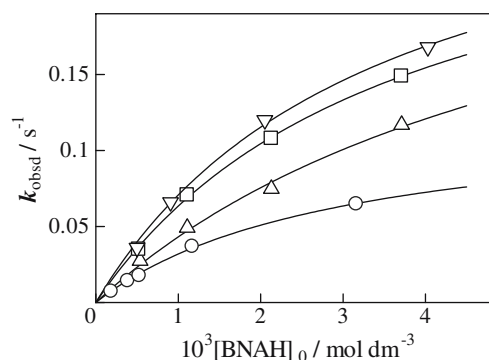


Figure 2. Plots of the observed rate constant ( $k_{\text{obsd}}$ ) vs. BNAH concentration for the reaction of  $\text{MB}^+$  with BNAH in 10% ethanol-90% water mixed solvent at 298 (○), 303 (△), 308 (□) and 313 K (▽).

reaction of  $\text{MB}^+$  with BNAH obeyed a first-order rate law in the presence of excess BNAH.

The apparent first-order rate constants ( $k_{\text{obsd}}$ ) were obtained with several concentrations of BNAH at various temperatures. Saturation curves were obtained by plotting the  $k_{\text{obsd}}$  values against  $[\text{BNAH}]_0$  at each temperature (Figure 2). The dependence of  $k_{\text{obsd}}$  on  $[\text{BNAH}]_0$  can be described by

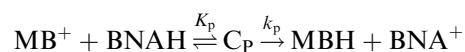
$$k_{\text{obsd}} = \frac{a[\text{BNAH}]_0}{1 + b[\text{BNAH}]_0} \quad (6)$$

where  $a$  and  $b$  are parameters discussed later.

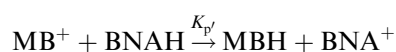
Equation (6) can be rewritten as

$$\frac{[\text{BNAH}]_0}{k_{\text{obsd}}} = \frac{1}{a} + \frac{b}{a}[\text{BNAH}]_0 \quad (7)$$

This equation is verified by plots of  $[\text{BNAH}]_0/k_{\text{obsd}}$  versus  $[\text{BNAH}]_0$ , which are straight lines as shown in Figure 3. The linearity of  $[\text{BNAH}]_0/k_{\text{obsd}}$  versus  $[\text{BNAH}]_0$  is characterized by a 1:1 complex formation between  $\text{MB}^+$  and BNAH which equilibrates much more rapidly than the hydride transfer between these species. Such a complex may be productive (Scheme A) or nonproductive (Scheme B) and these two possibilities are kinetically indistinguishable.



Scheme A



## Scheme B

In Scheme A, the complex ( $C_P$ ) is considered to be productive. From Scheme A,  $k_{\text{obsd}}$  is given by Equation (8).

$$k_{\text{obsd}} = \frac{k_P K_P [\text{BNAH}]_0}{1 + K_P [\text{BNAH}]_0} \quad (8)$$

which can be rewritten as Equation (9).

$$\frac{[\text{BNAH}]_0}{k_{\text{obsd}}} = \frac{1}{k_P K_P} + \frac{1}{k_P} [\text{BNAH}]_0 \quad (9)$$

In Scheme B, the complex ( $C_{NP}$ ) is considered to be a "bystander". From Scheme B,  $k_{\text{obsd}}$  is given by Equation (10).

$$k_{\text{obsd}} = \frac{k_{P'} [\text{BNAH}]_0}{1 + K_{NP} [\text{BNAH}]_0} \quad (10)$$

which can be rewritten as Equation (11).

$$\frac{[\text{BNAH}]_0}{k_{\text{obsd}}} = \frac{1}{k_{P'}} + \frac{K_{NP}}{k_{P'}} [\text{BNAH}]_0 \quad (11)$$

Equations (8) and (9) are kinetically indistinguishable from Equations (10) and (11), and Equations (9) and (11) predict a linear correlation between  $[\text{BNAH}]_0/k_{\text{obsd}}$  and  $[\text{BNAH}]_0$ . This agrees fairly well with the results obtained (Figure 3).

As mentioned above, for only the reactions which activation enthalpies were negative, we could conclude that CT complexes act as real intermediates. In this study we investigated the temperature dependence of the rate of the hydride transfer reaction between  $\text{MB}^+$  and BNAH.

As shown in Figure 2, saturation curves were obtained by plotting the  $k_{\text{obsd}}$  values against BNAH concentration at various temperature. Figure 3 shows the plots of  $1/k_{\text{obsd}}$  against  $1/[\text{BNAH}]$ .

The values of  $k_P$  ( $k_{NP}/K_{NP}$ ),  $K_P$  ( $K_{NP}$ ) and  $k_P K_P$  ( $k_{NP}$ ) at various temperatures can be obtained from the intercepts and the slopes of straight lines in Figure 3. Figure 4 shows the Arrhenius and van't Hoff plots of  $k_P$  ( $k_{NP}/K_{NP}$ ),  $K_P$  ( $K_{NP}$ ) and  $k_P K_P$  ( $k_{NP}$ ). The activation

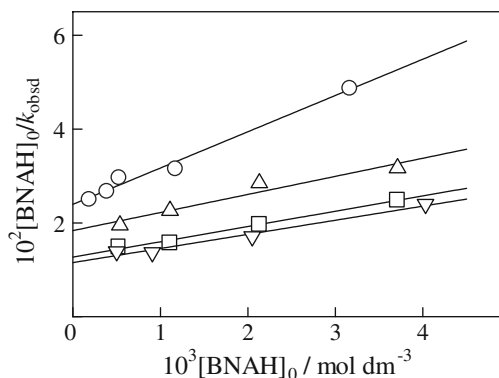


Figure 3. Plots of  $[\text{BNAH}]_0/k_{\text{obsd}}$  vs.  $[\text{BNAH}]_0$  for the reaction of  $\text{MB}^+$  with BNAH in 10% ethanol-90% water mixed solvent at 298 (O), 303 (Δ), 308 (□) and 313 K (∇).

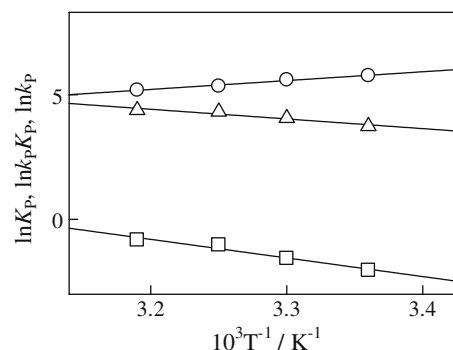


Figure 4. Arrhenius and van't Hoff plots of  $k_P K_P$  (or  $k_{P'}$ ) (Δ),  $k_P$  (or  $k_{P'}/K_{NP}$ ) (O) and  $K_P$  (or  $K_{NP}$ ) (□) for the reaction of  $\text{MB}^+$  with BNAH in 10% ethanol-90% water mixed solvent.

and reaction enthalpies for  $k_P$  (or  $k_{NP}/K_{NP}$ ),  $K_P$  (or  $K_{NP}$ ) and  $k_P K_P$  (or  $k_{NP}$ ) were obtained ( $\Delta H_1^\ddagger = 65.2$  for  $k_P$  (or  $k_{NP}/K_{NP}$ ),  $\Delta H_2^\ddagger = -30.7$  for  $K_P$  (or  $K_{NP}$ ) and  $\Delta H_3^\ddagger = 34.5$   $\text{kJ mol}^{-1}$  for  $k_P K_P$  ( $k_{NP}$ )). Since the positive apparent activation enthalpy for  $k_P K_P$  ( $k_{NP}$ ) was obtained, Scheme A and B could not be distinguished from the temperature dependence of the rate of the hydride transfer reaction from BNAH to  $\text{MB}^+$ .

#### Effect of $\beta$ -CD on the hydride transfer reaction between BNAH and $\text{MB}^+$

For  $\beta$ -CD, details of inclusion complexation with many kinds of guest molecules and their actions on the reactions (effects on both the equilibrium and rate constants) have been examined extensively. In general, inhibition of bimolecular reactions by  $\beta$ -CD is due to separation of the reactants, that is, only one reactant can fit into the CD cavity, or two reactants are separately included by two cavities.

Figure 5 illustrates the changes in  $k_{\text{obsd}}$  with  $\beta$ -CD concentration. As shown in Figure 5, the reaction between BNAH and  $\text{MB}^+$  was retarded by the addition of  $\beta$ -CD. This is due to separation of the reactants by  $\beta$ -CD, that is, for  $\text{MB}^+$  (and BNAH) included in the cavity of  $\beta$ -CD.

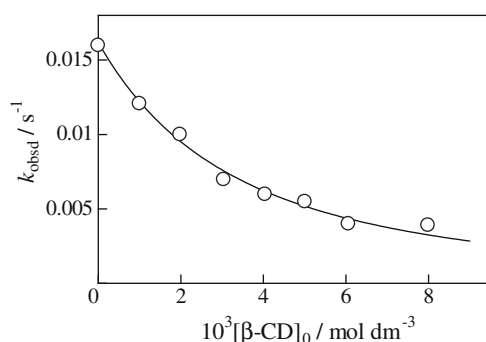


Figure 5. Effect of  $\beta$ -CD on the observed rate constant ( $k_{\text{obsd}}$ ) for the reaction of  $\text{MB}^+$  with BNAH in 10% ethanol-90% water mixed solvent at 298 K.

The addition of  $\beta$ -CD to  $\text{MB}^+$  and BNAH solutions in 10% ethanol-90% water mixed solvent caused changes in their absorption spectra. Although the spectral changes were small, the rough values of the equilibrium constants for the formation of 1:1 complexes between  $\text{MB}^+$  (BNAH) and  $\beta$ -CD could be obtained. The values obtained for  $\text{MB}^+$  and BNAH were 130 and  $220 \text{ dm}^3 \text{ mol}^{-1}$ , respectively. These values were considerably smaller than those obtained for the formation of 1:1 complexes between  $\text{MB}^+$  (BNAH) and  $\beta$ -CD in aqueous solution (values of 420 [19] and  $460 \text{ dm}^3 \text{ mol}^{-1}$  [29] for  $\text{MB}^+$  and  $810 \text{ dm}^3 \text{ mol}^{-1}$  for BNAH [30] were reported).

Taking into account the formation of the complexes of BNAH and  $\text{MB}^+$  with  $\beta$ -CD and assuming that these inclusion complexes does not react with each other, nor with free reactants, the following equation can be obtained.

$$k_{\text{obsd}} = \frac{k_{\text{app}}}{(1 + K_1[\beta - \text{CD}])(1 + K_2[\beta - \text{CD}])} \quad (12)$$

where  $k_{\text{app}}$  is the apparent rate constant in the absence of  $\beta$ -CD with same initial concentration of BNAH.

The solid line in Figure 4 shows the values calculated by Equation (9) using  $K_1 = 130 \text{ dm}^3 \text{ mol}^{-1}$  and  $K_2 = 220 \text{ dm}^3 \text{ mol}^{-1}$ . As shown in Figure 5, the agreement between observed and calculated values is good. In this reaction,  $\text{MB}^+$  and BNAH were separately included in the cavities of different  $\beta$ -CDs, and the cavity walls may protect the activity sites of the reactants.

Previously we observed that the mixed surfactant systems of cationic or anionic surfactants with nonionic surfactants have inhibition effects on the hydride transfer reaction between leuco methylene blue and 2,5-dihydroxy-1,4-benzoquinone [31]. These effects were attributed to the effect induced by the absorption of one of substrates on mixed micelles.

#### *Effect of $\gamma$ -CD on the hydride transfer reaction between BNAH and $\text{MB}^+$*

It is well known that equilibrium between the  $\text{MB}^+$  monomer and its dimer exists in aqueous solution. The absorption spectrum of  $\text{MB}^+$  was found to depend on the concentration of  $\text{MB}^+$  also in 10% ethanol-90% water mixed solvent. This showed the formation of  $\text{MB}^+$  dimer in regions of high concentration. The equilibrium constant obtained for the dimerization of  $\text{MB}^+$  was  $4300 \text{ mol dm}^{-3}$ . This value is smaller than that reported value for  $\text{MB}^+$  dimerization in aqueous solution ( $9600 \text{ mol dm}^{-3}$  [28]).

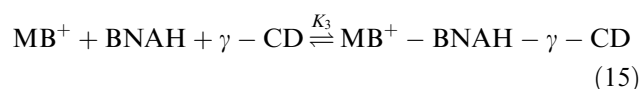
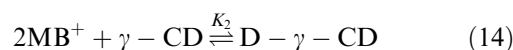
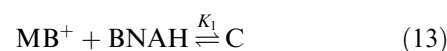
Judging from the equilibrium constant, only 4% of  $\text{MB}^+$  exists as the dimer under the present conditions ( $[\text{MB}^+]_0 = 1.0 \times 10^{-5} \text{ mol dm}^{-3}$  in 10% ethanol-90% water mixed solvent). As described above,  $\beta$ -CD stabilized the monomer and the dimer proportion in solutions further decreased in the presence of  $\beta$ -CD. Thus, existence of the dimer was negligible in 10%

ethanol-90% water mixed solvent and in the presence of  $\beta$ -CD.

On the other hand, a decrease in the  $\text{MB}^+$  monomer peak (664 nm) with a concomitant increase in the  $\text{MB}^+$  dimer peak (604 nm) with an isosbestic point at 623 nm was clearly observed by adding  $\gamma$ -CD to the solution, as illustrated in the literature [19]. This indicated that the  $\text{MB}^+$  dimer was included and stabilized in the cavity of  $\gamma$ -CD. This shows that in the presence of  $\gamma$ -CD the existence of the dimer species can not be neglected.

Tan *et al.* [23] and Hamai and Satou [19] found that a ternary 1:1:1 complex formed between  $\gamma$ -CD and some organic ions. Although the evidence of ternary 1(1(1 complex formation among BNAH,  $\text{MB}^+$  and  $\gamma$ -CD could not be obtained, because the hydride transfer reaction between  $\text{MB}^+$  and NDAH is too fast, the Corey-Pauling-Koltum model analysis showed that the dimension of the  $\gamma$ -CD cavity was suitable to include both BNAH and  $\text{MB}^+$  simultaneously. The  $\gamma$ -CD cavity was too large to form stable inclusion complexes with the monomer of  $\text{MB}^+$  and BNAH.

As mentioned above, the  $\text{MB}^+$  dimer is stabilized in the cavity of  $\gamma$ -CD. Furthermore, in the  $\text{MB}^+$ -BNAH- $\gamma$ -CD system, the formation of a ternary 1:1:1 complex among them is also possible. In this case,  $\text{MB}^+$  exists as the species shown by the following reactions in the reaction mixtures in the presence of  $\gamma$ -CD.



The absorbance at the  $\text{MB}^+$  monomer peak (664 nm) is expressed as follows:

$$\begin{aligned} A &= \epsilon_{\text{M}}[\text{MB}^+] + \epsilon_{\text{C}}[\text{C}] + \epsilon_{\text{D}}[\text{D} - \gamma - \text{CD}] \\ &\quad + \epsilon_{\text{M}'}[\text{MB}^+ \cdot \text{BNAH} \cdot \gamma - \text{CD}] \\ &= (\epsilon_{\text{M}} + \epsilon_{\text{C}}K_1[\text{C}] + \epsilon_{\text{D}}K_2[\gamma - \text{CD}]_0)[\text{MB}^+] \\ &\quad + \epsilon_{\text{M}'}K_3[\text{BNAH}]_0[\gamma - \text{CD}]_0[\text{MB}^+] \\ &= B[\text{MB}^+] \end{aligned} \quad (16)$$

where  $\epsilon_{\text{M}}$ ,  $\epsilon_{\text{C}}$  and  $\epsilon_{\text{M}'}$  are the molar absorption coefficients of the  $\text{MB}^+$  monomer, the complex and the ternary complex ( $\text{MB}^+$ -BNAH- $\gamma$ -CD), respectively; and  $\epsilon_{\text{D}}$  is that of the  $\text{MB}^+$  dimer complex (D- $\gamma$ -CD) at 664 nm. Since the initial concentrations of BNAH and  $\gamma$ -CD are at least 10-fold larger than that of  $\text{MB}^+$ ,  $B$  depends only on  $[\text{MB}^+]$ . In the early stages of the reaction (for example, when the reaction extent is less than 20%),  $B$  can be assumed to be nearly constant. Therefore, the

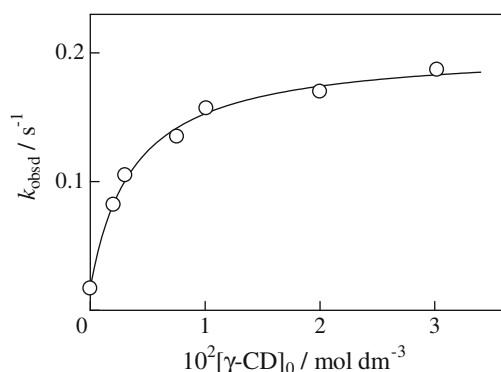


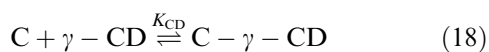
Figure 6. Effect of  $\gamma$ -CD on the observed rate constant ( $k_{\text{obsd}}$ ) for the reaction of  $\text{MB}^+$  with BNAH in 10% ethanol-90% water mixed solvent at 298 K.

rate of the decrease in absorbance at 664 nm is expressed as follows:

$$-\frac{dA}{dt} = -B \frac{d[\text{MB}^+]}{dt} = Bk_{\text{obsd}}[\text{MB}^+] = k_{\text{obsd}}A \quad (17)$$

In this case, the decrease in  $A$  with reaction time can be regarded as a first-order decay. The absorbance-time data within the 20% reaction extent were fitted by a first-order integrated equation, and the values of the pseudo-first-order rate constant ( $k_{\text{obsd}}$ ) for various concentration of  $\gamma$ -CD were obtained.

As shown in Figure 6, the  $k_{\text{obsd}}$ -value increases with increasing  $\gamma$ -CD concentration. If the 1:1:1 ternary complex among  $\text{MB}^+$ , BNAH and  $\gamma$ -CD can be assumed to the inclusion complex of the complex (C) between  $\text{MB}^+$  and BNAH, it is possible to distinguish between two mechanisms for the reaction of  $\text{MB}^+$  with BNAH (Scheme A and B shown above). For Scheme A, the following reactions (18) and (19) must be added to the mechanism to discuss the effect of  $\gamma$ -CD on the rate, and for Scheme B, only reaction (18) has to be added to the mechanism.



From Scheme A and reactions (18) and (19),  $k_{\text{obsd}}$  is given by Equation (20)

$$k_{\text{obsd}} = \frac{(k_{\text{p}}K_{\text{P}} + k'_{\text{p}}K_{\text{P}}K_{\text{CD}}[\gamma - \text{CD}]_0)[\text{BNAH}]_0}{1 + K_{\text{P}}[\text{BNAH}]_0 + K_{\text{P}}K_{\text{CD}}[\text{BNAH}]_0[\gamma - \text{CD}]_0} \quad (20)$$

On the other hand, from Scheme B and reaction (18),  $k_{\text{obsd}}$  is given by Equation (21)

$$k_{\text{obsd}} = \frac{k'_{\text{p}}[\text{BNAH}]_0}{1 + K_{\text{NP}}[\text{BNAH}]_0 + K_{\text{NP}}K_{\text{CD}}[\text{BNAH}]_0[\gamma - \text{CD}]_0} \quad (21)$$

Equations (20) and (21) indicate that Scheme A and B show the opposite effect of  $\gamma$ -CD on  $k_{\text{obsd}}$ , that is, in Scheme A,  $\gamma$ -CD enhances the hydride transfer reaction and in Scheme B, it suppresses the reaction. As shown in Figure 6, the  $k_{\text{obsd}}$ -value increased with increasing  $\gamma$ -CD concentration.

The values of the kinetic and thermodynamic parameters in Equation (20) were determined by a nonlinear least-squares curve-fitting method. The fitting of the experimental data with Equation (20) indicated that Scheme A was valid. The values of the equilibrium constant  $K_{\text{P}}$  and rate constant  $k_{\text{P}}$  obtained above were used as known constants. The  $K_{\text{CD}}$  and  $k'_{\text{p}}$  values obtained by curve-fitting were  $2700 \text{ dm}^3 \text{ mol}^{-1}$  and  $0.11 \text{ s}^{-1}$ . The evaluated value of  $k'_{\text{p}}$  is in good agreement with that of  $k_{\text{P}}$ , revealing that the reactivity of the complex (C) in the cavity of  $\gamma$ -CD is similar to that of the free complex (C). This shows that the assumption that the 1:1:1 ternary complex among  $\text{MB}^+$ , BNAH and  $\gamma$ -CD is the inclusion complex of C is valid.

Although in the present reaction system, there was no spectroscopic evidence of the formation of a complex during the reaction of  $\text{MB}^+$  with BNAH and the stabilization of the complex by  $\gamma$ -CD, enhancement of the reaction by  $\gamma$ -CD was observed. As mentioned above, this enhancement of the reaction can be explained by the formation of the inclusion complex of the productive complex between  $\text{MB}^+$  and BNAH. Therefore, the enhancement of the reaction observed in the present reaction system must indicate that the complex acts as a real intermediate.

It is possible that the effects of  $\gamma$ -CD on the rate of the hydride transfer reaction suggest another ways by which we can distinguish between the productive (Mechanism-1) and non-productive (Mechanism-2) nature of the complex in some cases. This study shows that the inclusion phenomenon into CD can provide conclusive information on the reaction mechanism.

## Reference

1. K.A. Connors: *Chem. Rev.* **97**, 1325 (1997).
2. E. Iglosias and A. Fernandez: *J. Chem. Soc., Perkin Trans.* **2**, 1691 (1998).
3. L. Garcia-Rio, J.R. Leis, J.C. Mejuto, and J. Perez-Juste: *J. Phys. Chem.* **101**, 7383 (1997).
4. R.M.G. Roberts, D. Ostovic, and M.M. Kreevoy: *Faraday Discuss., Chem. Soc.* **74**, 257 (1982).
5. I.H. Lee, E.H. Jeovrg, and M.M. Kreevoy: *J. Am. Chem. Soc.* **119**, 2722 (1997).
6. A. Ohno: *J. Phys. Org. Chem.* **8**, 567 (1995).
7. N.S. Isaacs, K. Javid, and E. Rannala: *Nature* **268**, 372 (1977).
8. A. Ohno, T. Shio, H. Yamamoto, and S. Oka: *J. Am. Chem. Soc.* **103**, 2045 (1981).
9. A.K. Colter, C.C. Lai, T.W. Williamson, and R.E. Berry: *Can. J. Chem.* **61**, 2544 (1983).
10. S. Fukuzumi, N. Nishizawa, and T. Tanaka: *J. Org. Chem.* **49**, 3571 (1984).
11. S. Yamamoto, Y. Fujiyama, M. Shiozaki, Y. Sueishi, and N. Nishimura: *J. Phys. Org. Chem.* **8**, 805 (1995).
12. Y. Liu, S. Yamamoto, and Y. Sueishi: *J. Phys. Org. Chem.* **12**, 194 (1999).

13. J.W. Bunting, W.S.F. Chew, and G. Chu: *J. Org. Chem.* **42**, 2303 (1982).
14. V.D. Kiselev and J.G. Miller: *J. Am. Chem. Soc.* **97**, 4036 (1975).
15. K.M. Zaman, S. Yamamoto, N. Nishimura, J. Maruta, and S. Fukuzumi: *J. Am. Chem. Soc.* **116**, 12099 (1994).
16. S. Yamamoto, T. Sakurai, Y. Liu, and Y. Sueishi: *Phys. Chem. Chem. Phys.* **1**, 833 (1999).
17. S. Fukuzumi, K. Ohkubo, Y. Tokuda, and T. Suenobu: *J. Am. Chem. Soc.* **122**, 4286 (2000).
18. A. Ueno, K. Takahashi, and T. Osa: *J. Chem. Soc. Comm.*, 921 (1980).
19. S. Hamai and H. Satou: *Bull. Chem. Soc. Jpn.* **73**, 2207 (2000).
20. H. Hirai, N. Toshima, and S. Uenoyama: *Bull. Chem. Soc. Jpn.* **58**, 1156 (1985).
21. E.K. Fraiji, T.R. Gregan Jr., and T.C. Werner: *Appl. Spectrosc.* **48**, 79 (1994).
22. R.L. Schiller, S.F. Lincoln, and J.H. Coates: *J. Chem. Soc., Faraday Trans.* **1**(80), 3119 (1984).
23. W.H. Tan, T. Ishikura, A. Maruta, T. Yamamoto, and Y. Matsui: *Bull. Chem. Soc. Jpn.* **71**, 2323 (1998).
24. S. Hamai: *Bull. Chem. Soc. Jpn.* **73**, 861 (2000).
25. S. Hamai and H. Satou: *Bull. Chem. Soc. Jpn.* **75**, 77 (2002).
26. P. Sevcik and H.B. Dunford: *J. Phys. Chem.* **95**, 2411 (1991).
27. M. Marazona, G. Giraudi, and P. Carraro: *Ann. Chim.* **82**, 39 (1992).
28. C. Lee, Y.W. Sung, and J.W. Park: *J. Phys. Chem. B* **103**, 893 (1999).
29. G. Zhang, S. Shuang, C. Dong, and J. Pan: *Spectrochim. Acta, Part A* **59**, 2935 (2003).
30. T.A. Gadosy and O.S. Tee: *Can. J. Chem.* **74**, 745 (1996).
31. B. Jiang, S. Cheng, X. Zeng, Y. Liu, S. Yamamoto, and Y. Sueishi: *J. Disper. Scie. Technol.* **24**, 691 (2003).